

Numerical formulation of P-I diagrams for blast damage prediction and safety assessment of RC panels

Mohamed H. Mussa^{*1,2}, Azrul A. Mutalib¹ and Hong Hao³

¹Department of Civil Engineering, Faculty of Engineering & Built Environment, Universiti Kebangsaan Malaysia, 43600 UKM Bangi, Selangor, Malaysia

²Department of Civil Engineering, University of Warith Al-Anbiyaa, 56001 Karbala, Iraq,

³Centre for Infrastructural Monitoring and Protection, School of Civil and Mechanical Engineering, Curtin University, Kent Street, WA 6102, Australia

(Received December 17, 2018, Revised March 28, 2020, Accepted April 3, 2020)

Abstract. A numerical study is carried out to assess the dynamic response and damage level of one- and two-way reinforced concrete (RC) panels subjected to explosive loads by using finite element LS-DYNA software. The precision of the numerical models is validated with the previous experimental test. The calibrated models are used to conduct a series of parametric studies to evaluate the effects of panel wall dimensions, concrete strength, and steel reinforcement ratio on the blast-resistant capacity of the panel under various magnitudes of blast load. The results are used to develop pressure-impulse (P-I) diagrams corresponding to the damage levels defined according to UFC-3-340-02 manual. Empirical equations are proposed to easily construct the P-I diagrams of RC panels that can be efficiently used to assess its safety level against blast loads.

Keywords: P-I curves; RC panels; blast load; numerical formulation; damage assessment

1. Introduction

Several RC panels are designed as an efficient bracing system that offers a great potential for both lateral load resistance and drift control, however, most of these structures are not designed to resist blast loads (Shen *et al.* 2010, Ha *et al.* 2011). These panels might be exposed to blast loadings generated either accidentally or hostile by terrorist attacks (Ngo *et al.* 2007). Therefore, the failure of those panels could cause great losses in lives and infrastructures. Consequently, it is essential to provide a clear assessment of the performance and protection levels of RC panels under this type of loads.

Experimental studies had been conducted to investigate the behaviour of RC panel under blast loads. The results revealed that these loads can result in structural damage in the forms of shear and flexural failure, as well as a localized crushing, spalling and scabbing damage. As an instance, the field test of an RC wall carried by Gebbeken and Ruppert (1999), whereas the wall was severely damaged by direct shear under a close-in explosion of 6000 kg TNT due to the high impact velocity. Ngo (2005) tested the response of one-way panel under an average reflected impulse and pressure of 2876kPa.ms and 735kPa, respectively. The results indicated that the panel failed in a flexural mode which was observed from the vertical mid-span crack on the front and rear surfaces. Similar failure mode was observed by Riedel *et al.* (2010) during the test of a panel under peak

pressure and impulse of 208kPa and 3038kPa.ms, respectively. Otherwise, Muszynski and Purcell (2003) observed that the tested panel failed in tension failure under an explosive charge weight of 830 kg detonated at 14.6m standoff distance from the structure. Based on previous test results, RC panels may fail with various modes depending on the structure and explosion conditions. Therefore, a comprehensive evaluation of structural damage should be considered taking into account the effects of both the blast loading amplitude and duration on structure responses. One of the simplest approaches to correlate the duration of blast pressure along with its amplitude to reach a particular damage level of the structural component is by using Pressure-Impulse (P-I) diagrams.

Several methods such as analytical, numerical and experimental had been proposed to develop the P-I diagrams of RC members. The single degree of freedom (SDOF) method is commonly used to derive the P-I diagrams, whereas a computer program FACEDAP (Oswald and Marchand 1994) is developed according to this approach and widely adopted by scholars. However, one challenge is distinguished in utilizing the SDOF approach is to acquire a reliable resistance function for a structure due to the kinds of resistance function adopted in the derivation of the equivalent SDOF system could considerably influence on the ultimate response of concrete elements and the amount of blast damage (Saadun *et al.* 2016, Mussa *et al.* 2018). Syed *et al.* (2006) reported the effects of using bilinear and nonlinear resistance functions in the derivation of an equivalent SDOF system for RC panels. The results showed that the post-peak response is significantly varied when different functions are applied. In the same context, Shope (2007) utilized a yield line theory to derive P-I

*Corresponding author, Ph.D.

E-mail: eng.mhmussa@siswa.ukm.edu.my or
dr.mhmussa@uowa.edu.au; azrulaam@ukm.edu.my

diagrams of RC walls. The results revealed a good consistency with the P-I diagrams obtained according to SDOF method. The SDOF approach is handy to assess the behaviour of the structural member under blast loads including the combined shear and flexural failure (Krauthammer *et al.* 2008, Hou *et al.* 2018, Yu *et al.* 2019). Nevertheless, some difficulties are highlighted by using this approach in the prediction of localized failure. Recently, the numerical approach showed a good capability to give a reliable prediction to the behaviour of RC structure under blast loads (Mussa *et al.* 2017, Mutalib *et al.* 2020). This approach does not need to define a resistance function; nevertheless, complex dynamic material properties could be taken into consideration and various failure modes could be detected including crushing and spalling failure that considered difficult to be reliably modelled by an equivalent SDOF system (Mussa *et al.* 2018). The numerical approach had successfully overcome the limitations of the simplified SDOF model (Abbood *et al.* 2018). Consequently, numerous scholars had adopted this approach to study the dynamic response of various RC structures such as columns (Abedini *et al.* 2017, Mutalib *et al.* 2018), slabs (Xia *et al.* 2014, Mussa *et al.* 2020), and walls (Aghdamy *et al.* 2013, Sohn *et al.* 2014). For panels, Lin *et al.* (2014) used LS-Dyna software to study the effects of TNT charge weight, standoff distance, panel thickness and steel reinforcement ratio on the blast resistance of RC panels. The results proved that the deformation of panels can be reduced by increasing the panel thickness and the steel reinforcement ratio. Christian and Chye (2014) used LS-Dyna to evaluate the performance of fibre reinforced plastic (FRP) composite panel as compared to a conventional steel concrete steel (SCS) panel and an ordinary RC panel. The results proved that the combination of FRP and cellular steel sandwich could utilize as a blast mitigation panel owing to its high energy absorption properties. Lee and Kim (2016) conducted a comparative study between blast-resistant of steel-plate concrete (SC) and RC panels by using LS-Dyna software. The results indicated that the SC panel has a superior impact resistance than RC panel; therefore the concrete thickness and steel ratio of SC panel was greatly reduced as compared with those of the RC panel. Lin and Zhang (2016) investigated the effects of FRP thickness, retrofitted surface, standoff distance and the charge mass on the blast resistance of the RC panel by using LS-Dyna software. The results indicated that the increase of FRP could significantly decrease the maximum and residual deflections of RC panel. In the same context, Mutalib *et al.* (2019) studied the effects of carbon fibre reinforced plastic (CFRP) strengthening on the RC panel resistance with and without anchoring against blast loads by using LS-Dyna software and the numerical outcomes are used to develop pressure-impulse (P-I) diagrams. In this field, the numerical derivation of P-I diagrams for RC panel subjected to blast loads is still limited. Parlin *et al.* (2014) used experimental and numerical approaches to evaluate the blast response of lightweight wall panels and developed P-I diagrams depending on the maximum deflection damage criterion. The pseudo-static bending tests were carried out to determine the load-deformation properties of the panel. The

P-I curves were developed by using both linear and nonlinear dynamic analysis and proved that these curves are a valuable tool for evaluating the panel damage under a variety of blast loads. Moreover, the results revealed that the behaviour of the panel's wall can be represented by a nonlinear SDOF model. Shi and Stewart (2015) successfully assessed the damage of RC panels exposed to blast loading by using the maximum support rotation (θ) obtained from the LS-DYNA analysis. Three damage levels were proposed according to specifications UFC-3-340-02 (2008). In this study, intensive numerical simulations are performed to investigate the dynamic response and develop P-I curves and equations for protection and prediction of panel damage with different RC wall dimensions, concrete strength (f_{cu}) and steel reinforcement ratio (ρ) subjected to various values of blast load. Damage criteria given in technical manual UFC-3-340-02 (2008) based on the support rotation are used in this study.

2. Numerical modelling

2.1 Geometrical details and boundary conditions

The numerical model of RC panel is created by using LS-DYNA software (LSTC 2012) according to a field test of the unstrengthened RC panel performed by Muszynski and Purcell (2003) as shown in Fig. 1. The ground and upper slabs, as well as the side concrete columns, are modelled, to represent the real scenario of RC panel during the field test. Smeared modelling was used to simulate the above parts. The nodes at the ground slab, the lower and upper column surface as well as on the side edges of the upper slab were fixed. An (Automatic Surface To Surface) contact is applied between the panel and the surrounded structures to avoid the penetration of the damaged panel material beneath the floor level. In the case of one-way panels, the movement of the nodes along the left and right sides of the RC wall was fixed in Y- direction. While in the case of two-way panels, the movement of the nodes was fixed at all sides of the panel wall in a similar direction.

2.2 Material model

The concrete with compressive strength of 30MPa is modelled by using the material model (72Rel3) available in LS-DYNA software with (MAT_Add_Erosion) (LSTC 2012). Previous studies showed that the use of a material model (72Rel3) provides an accurate and reliable prediction for the concrete structure behaviour under blast load (Malvar *et al.* 1997, Yonten *et al.* 2002). While material model 24 (MAT_Piecewise_Linear_Plasticity) is adopted to model the reinforcement steel which defined as an elastic-plastic material model that allows the user to input effective stress versus effective plastic strain curve and defining the strain rate effect on the yield stress (LSTC 2012). The material properties of steel reinforcement are shown in Table 1.

The results of convergence test demonstrated that the simulation of concrete via solid elements with a mesh size of (25 × 25 × 25)mm, and steel reinforcement by beam

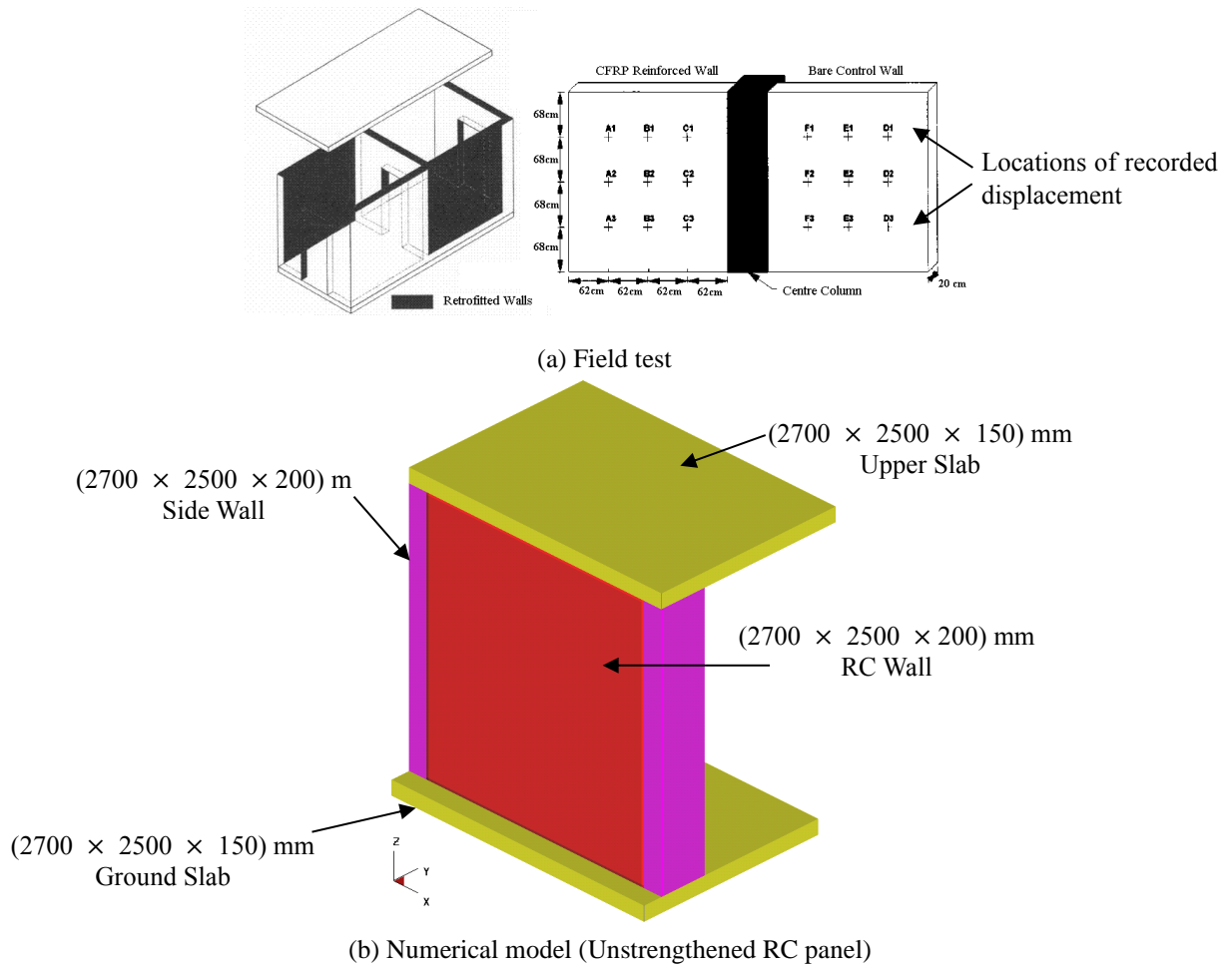


Fig. 1 Geometrical details

Table 1 Material properties of steel reinforcement

Properties	Concrete	Reinforcement
Mass density (kg/m^3)	2400	7800
Young modulus (GPa)	29	200
Poisson's ratio	0.2	0.3
Compressive strength (MPa)	30	-
Yield stress (MPa)	-	415

elements (2×2) Gauss quadrature integration with a mesh size of 25mm long (2-node Hughes-Liu) gave an accurate and reliable prediction for the behaviour of RC panels under blast load. In the current study, the bond-slip between reinforcement bars and concrete as defined by using CONTACT 1D. The bond between the steel bar and concrete is assumed as an elastic-plastic relation and the maximum shear stress (τ_{max}) is calculated as follows:

$$\tau_{max} = G_s u_{max} e^{-h_{dmg} D} \quad (1)$$

where G_s is the bond shear modulus, u_{max} is the maximum elastic slip, h_{dmg} is the damage curve exponent, and D is the damage parameter defined as the summation of the absolute values of the plastic displacement increments. Shi *et al.* (2009) conducted a series of parametric analysis and concluded that the effect of h_{dmg}

and D values is insignificant and might be ignored. In this study, G_s and u_{max} are taken as 20MPa/mm and 1.0mm, respectively, according to the recommendations proposed by Shi *et al.* (2009). The yield strength (f_y) of reinforcement steel is assumed to be 550MPa in the analysis. When different yield strength is used, the Equation (2) can be utilized to calculate the equivalent steel area (A_{se}):

$$A_{se} = \frac{f_y}{550} A_s \quad (2)$$

The Dynamic Increase Factor (DIF) of concrete in tension and compression were defined by using empirical equations of Malvar and Ross (1998) and CEB-FIP (1993) model, respectively. While for steel, the equation proposed by Malvar (1998) is utilized as shown in Fig. 2.

2.3 Simulation of blast loading

An explosive charge weight (W) of 830 kg TNT is exploded at a standoff distance (R) of 14.6 m from the structure during the field test carried by Muszynski and Purcell (2003). In this study, the negative phase of blast load is ignored and the positive phase is idealized as a triangular load. UFC-3-340-02 (2008) provided charts to determine the peak pressure and duration of blast load

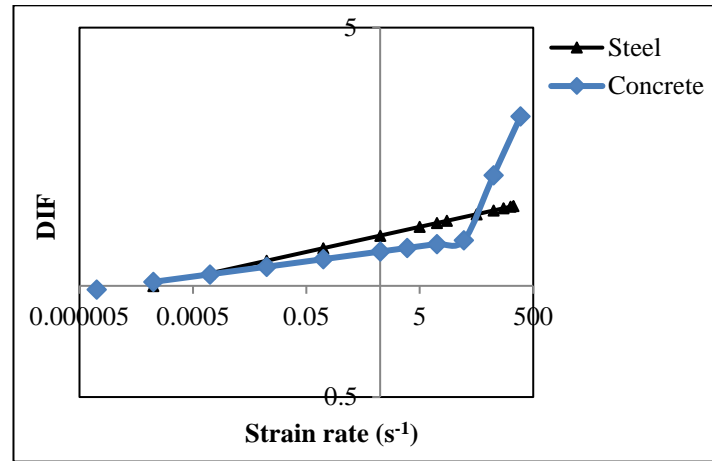


Fig. 2 DIF curves of concrete and steel reinforcement

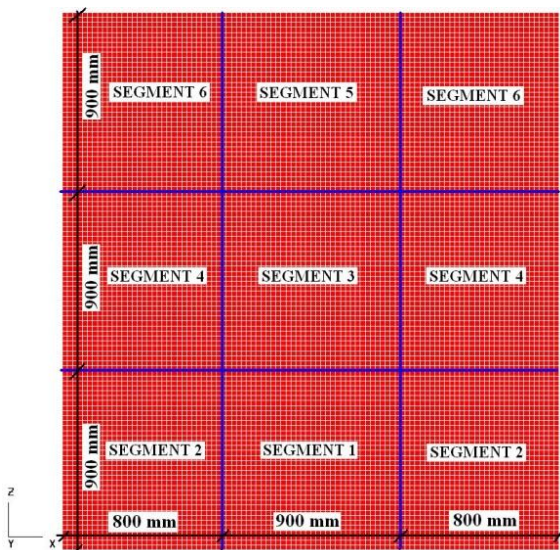


Fig. 3 Segmentation of RC panel to calculate the time history of blast load

acting on the structures in terms of the scaled distance ($Z = R/W^{1/3}$) and incident angle. Wu and Hao (2005) proved that the assumption of uniform pressure acting on the whole RC wall could cause a significant error when the scaled distance is less than 2. Hence, the wall of RC panels is divided into segments to calculate the pressure-time history of blast load as shown in Fig. 3.

The smaller segmentation is the most preferable to increase the estimation accuracy of blast pressure, however, too many segments might increase the computation time and cost. The pressure of blast load within each segment is considered a uniform and calculated via considered the centre point of the segment as a reference point in determining the stand-off distance and incident angle.

3. Validation of the numerical models

The accuracy of the numerical model was validated with the available field data of an RC panel tested under blast load by Muszynski and Purcell (2003). Two RC panels with and without CFRP strengthening were tested. In this paper,

Table 2 Residual displacement of unstrengthened RC Panel

Locations	Displacement (mm)		Differences (%)
	Experimental	Numerical	
D_1	25	26	4
D_2	34	28	18
D_3	39	29	26
E_1	30	39	30
E_2	52	67	29
E_3	52	50	4
F_1	22	22	0
F_2	36	29	19
F_3	39	26	33
Average	36.556	35.111	4
Std. deviation	9.912	13.812	-
CV	0.271	0.393	-

only the unstrengthened RC panel is simulated with dimensions of (2700 × 2500) mm reinforced by 9mm rebar at 300mm centre to centre spacing in both directions. Figure 4 and Table 2 showed a notable consistent between the numerical and experimental results in term of displacement at most of the investigated locations with an absolute average error of 4%. The obtained results revealed the capability of the numerical methods to determine the complex response of RC panels exposed to detonations within a short time and less cost. Furthermore, flexural cracks developed at the middle span towards the corner of the panel wall are observed during the numerical analysis, which is identical to those observed during the experimental test as shown in Fig. 4. This observation further confirms the reliability of the numerical model to predict the dynamic response of RC panels subjected to blast loads.

4. The failure mechanism of RC panels under blast loads

In 1973s, Mendes and Opat (1973) reported that clamped plates and beams could fail in three modes – large inelastic deformation (Mode I), tearing (tensile failure) in

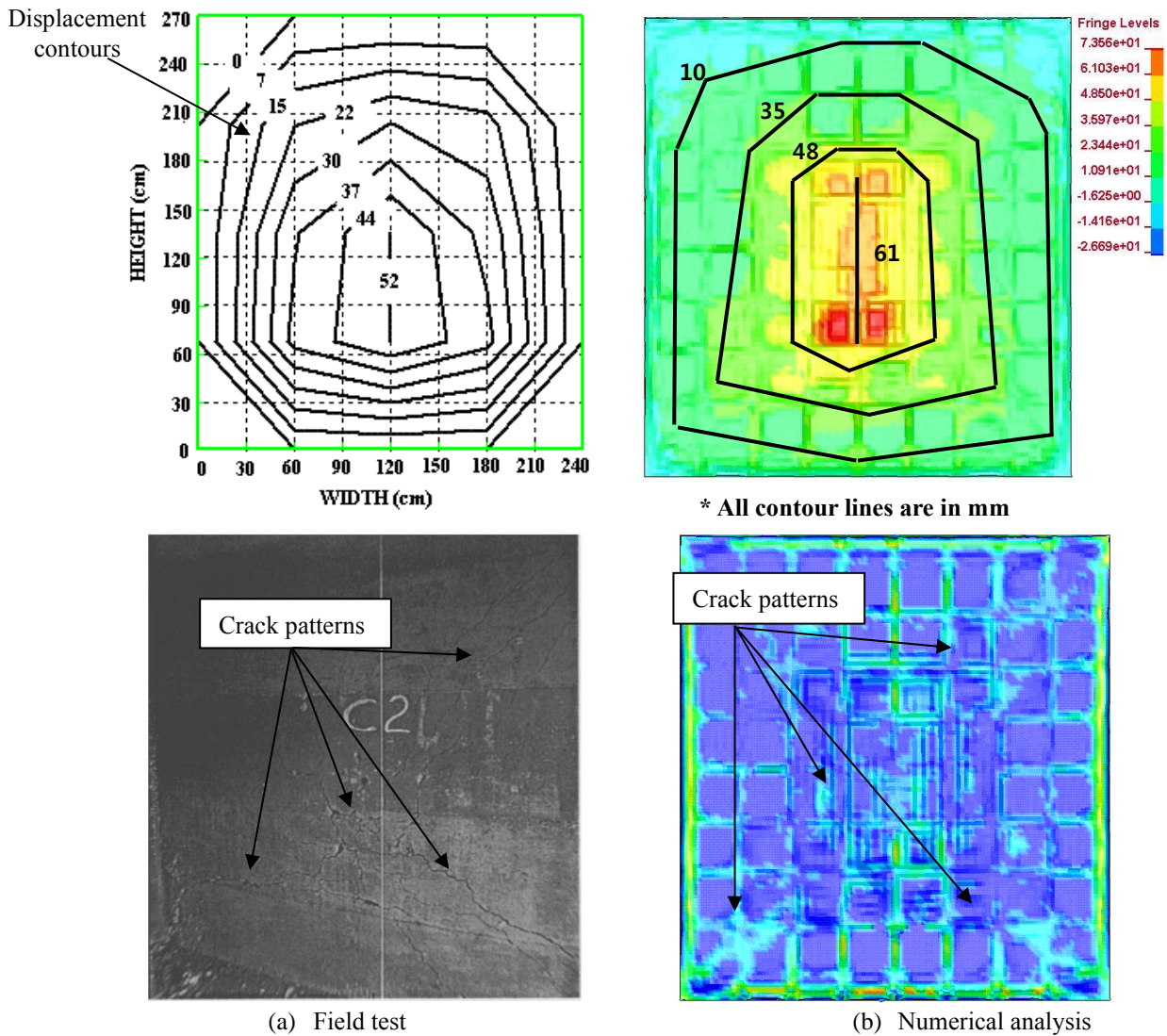


Fig. 4 Comparison of displacement contours and crack patterns after blasting

outer fibres or over the support (Mode II) and transverse shear failure (Mode III). The above failure modes were observed during the previous experimental tests conducted on circular and square steel plates (Krajcinovic 1972, Teeling-Smith and Nurick 1991, Olson *et al.* 1993, Nurick and Shave 1996, Mutalib *et al.* 2018). The RC panel might be damaged via a localized crushing or spalling when the explosion has occurred close to the structure. Otherwise, the panels are failed in similar patterns to those observed in case of steel plate. The failure mechanism of RC panels does not depend only on the pressure and duration of the blast loads but also depends on the boundary conditions and material properties of the panel. At the impulsive domain, the shear failure of the column was governed, while the flexural stress has no time to develop. On the other hand, the reduction of blast pressure value within the dynamic region domain and increase its impulse value resulted to appear the flexural failure, hence, a combination of shear and flexural failure of a column is observed at this region. At the quasi-static domain, the column is likely failed by flexural because of the peak pressure of blast load small but has a long duration.

Figure 5 showed that the failure mechanism might be varied in case of RC panels owing to the size of the panel surface to structure depth is comparatively higher than the RC column. Whereas, the shear failure (Mode I) of one- and two-way panels occurred at the impulsive region of 15000kpa and impulse of 2000 and 2400kpa.ms, respectively.

The reduction of blast pressure caused a clear decrease in shear failure and an obvious rise of flexural damage. Accordingly, both panels are failed by a combination of shear and flexural failure (Mode II) at a pressure of 5000kpa and impulses of 2100 and 3000kpa.ms, respectively. At the dynamic region, the deformation of both panels due to shear started to diminish and the flexural deflection becomes dominant owing to the negative bending moment and the absence of reinforcement in the front side of the panel. Thus, both panels suffered a predominantly flexural failure with tearing at the support (Mode III) when the pressure is reduced to 1000kpa and the impulse is increased to 2500 and 4500kpa.ms, respectively. The displacement at the midpoint of the one- and the two-way

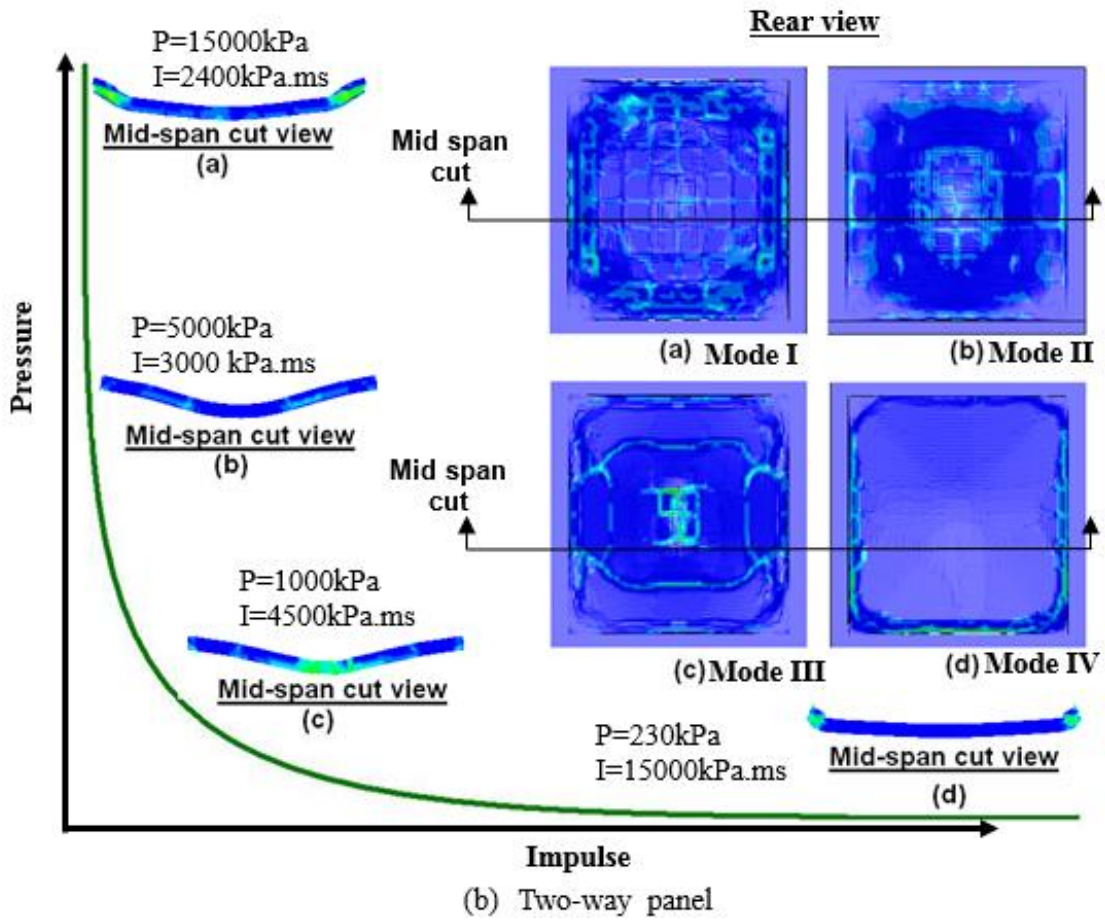
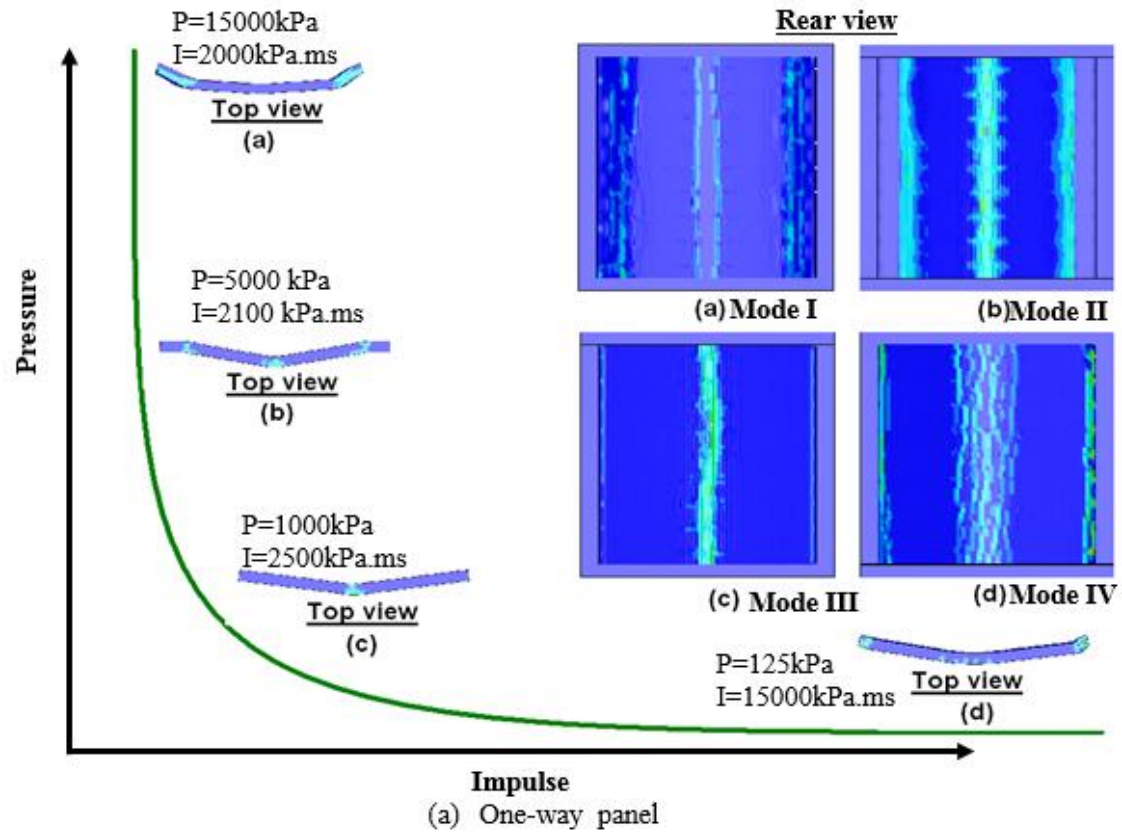


Fig. 5 Failure modes of one-and two-way RC panels after blasting

Table 3 Damage criteria of (UFC-3-340-02 2008)

Support Rotation (θ)	Damage Level
$\theta < 2^\circ$	Low damage (LD)
$2^\circ \leq \theta \leq 4^\circ$	Medium damage (MD)
$\theta > 12^\circ$	Severe damage (SD)

panels decrease within the quasi-static region when the pressure of detonation is further reduced to 125 and 230kpa, respectively, with the impulse of 15000kpa.ms, whereas the residual velocity caused an obvious transverse shear failure (Mode IV) at the support. The main difference between shear failure and transverse shear failure is the existence of the bending moment. The panel failed by shear when the moment did not induce, otherwise, the presence of bending moment resulted in normal stress as well as transverse shear stress which was greater than normal stress and resulted in panel failure at the support.

5. Damage criteria

Easy and appropriate damage criteria have to be utilized in the assessment of RC panels according to numerical results. FACEDAP (Oswald and Marchand 1994) stated that the damage can be evaluated in terms of qualitative and quantitative damage. However, the criterion of qualitative damage mainly relies on the reusable and repairable ability of the structure which is not easy to be determined by numerical analysis. On the other hand, the quantitative damage criteria considered more flexible and usually defined according to yield deflection at mid-span of the structural member. In the same context, UFC-3-340-02 (2008) used the quantitative damage and defined the criteria based on the support rotation (θ) of the members as shown in Table 3.

Shope (2007) used the maximum deflection (δ) corresponding to the support rotation (θ) to describe the damage level by using the following equation:

$$\delta = \frac{b}{2} \tan \theta \quad (3)$$

where b is the shortest panel span. In the current study, the value of (δ) is set to be the maximum mid-height deflection of the RC panel obtained from the numerical analysis to define the damage levels of P-I diagrams based on UFC-3-340-02 (2008) criteria.

6. Development of P-I diagrams

Several numerical simulations were performed by using LS-Dyna software to construct the P-I curves of one- and two-way RC panels corresponding to the damage levels suggested via UFC-3-340-02 (2008) under several magnitudes of blast load. During the simulation of one-way panels, the two sides of RC wall with depths of 150 and 200mm and steel ratios of 0.014 and 0.009, respectively, were clamped. While in the case of two-way panels, the four sides of the RC wall with width to height ratio of 0.6 to 1.4 were clamped.

 Table 4 Parameters of Equation (4) for one-way panels ($P1$ and $P2$)

panel	Damage level	P_0 (kPa)	I_0 (kPa)	A	β
$P1$	LD	100	1400	0.25	2.07
	MD	100	1500	0.25	2.06
	SD	100	1700	0.25	2.05
$P2$	LD	305	2000	0.25	2.19
	MD	305	2500	0.25	2.16
	SD	305	2800	0.25	2.14

 Table 5 Parameters of Equation (4) for two-way panels ($P3$ and $P4$)

Panel	Damage level	P_0 (kPa)	I_0 (kPa)	A	β
$P3$	LD	220	1600	0.25	2.07
	MD	220	2100	0.25	2.05
	SD	220	2800	0.25	2.03
$P4$	LD	520	2650	0.25	2.13
	MD	520	2900	0.25	2.13
	SD	520	3700	0.25	2.12

Figures 6 and 7 showed the good ability of the constructed curves to predict the damage levels of both panels within the dynamic region since the flexural failure is mainly dominated at this domain. However, the reliability of these curves was decreased when the blast pressure values within a quasi-static domain owing to the transverse shear failure of the panel is governed at this domain, while the adopted damage criteria of UFC-3-340-02 (2008) is based on the flexural deflection at the mid-span. Therefore, the P-I diagrams are converged to the same pressure asymptotes towards the quasi-static region as shown in Figs. 6 and 7. Scherbatyuk *et al.* (2008) observed a similar phenomenon during the numerical analysis of rigid-body rotation model, whereas all the P-I curves were converted to the same value at the quasi-static region due to the absence of a proper solution for a perfectly ideal step load that could allow the wall to acquire a maximum rotation between no rotations and complete overturning. Furthermore, the pressure capacity of the two-way panel was considerably higher as compared to the one-way panel within a comparable impulse asymptote.

An intensive empirical study was carried out to determine the best fitting for the numerical P-I curves of one- and two-way panels. The study revealed that these curves can be expressed analytically by a hyperbolic equation which is also been adopted via previous studies for columns and slabs (Oswald and Marchand 1994, Shope 2007, Shi *et al.* 2008, Mutalib and Hao 2011):

$$(P - P_0)(I - I_0) = A \left(\frac{P_0}{2} + \frac{I_0}{2} \right)^\beta \quad (4)$$

where P_0 and I_0 are the pressure and impulse asymptotes, respectively, A and β are constants determined via the best fitting method and mainly depend on the RC panel configuration and degree of damage as shown in Tables 4 and 5. The tendency of A and β coefficients for two-way RC panel are consistent with those observed by Shope (2007) that revealed the reliability of the proposed equation. The outcomes revealed a good agreement among the curves constructed by the numerical approach and empirical Equation (4) as described in Figs. 6 and 7.

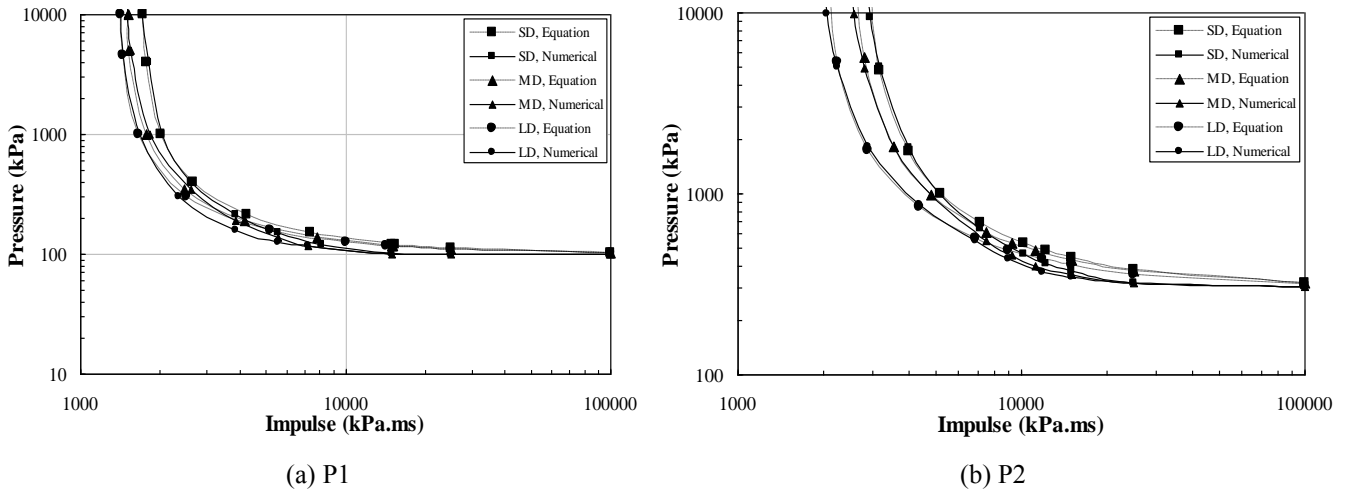


Fig. 6 P-I curves of one-way panels

4. Parametric studies

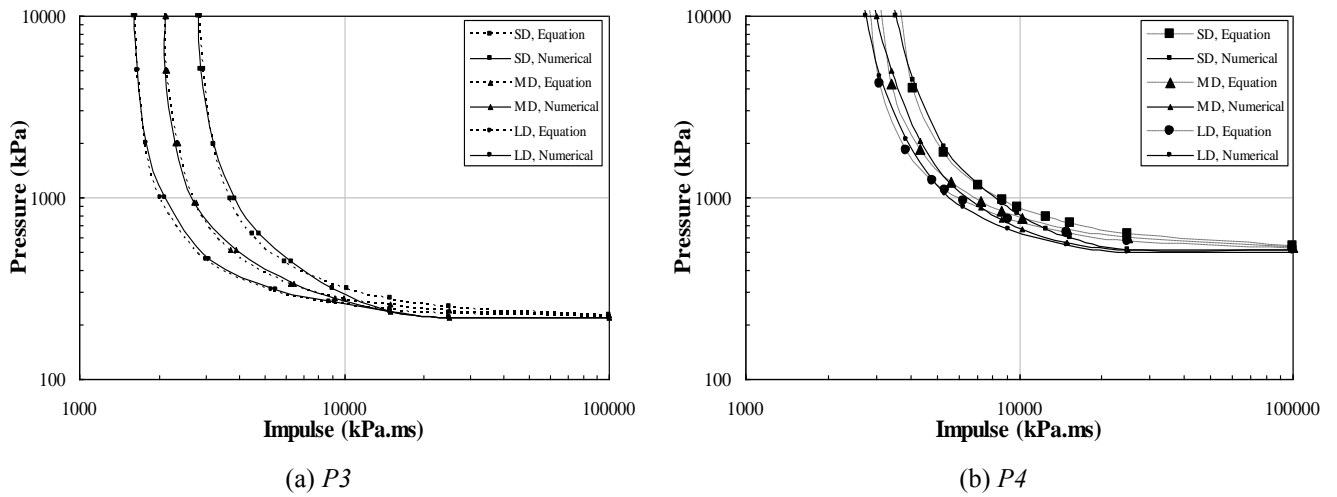


Fig. 7 P-I curves of two-way panels

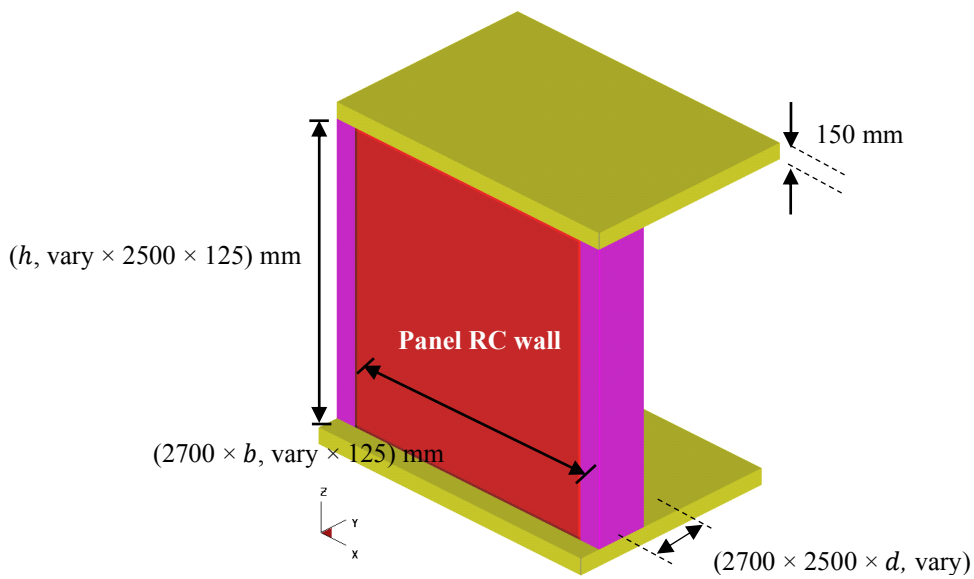


Fig. 8 Main variables in panel dimension during parametric studies

Table 6 Effect of panel depth (d) on the pressure and impulse of one- and two-way RC panels

Panel type	d (mm)	LD		MD		SD	
		P_0 (kPa)	I_0 (kPa.ms)	P_0 (kPa)	I_0 (kPa.ms)	P_0 (kPa)	I_0 (kPa.ms)
One-way	125	100	1400	100	1500	100	1700
	200	305	2000	305	2500	305	2800
	250	470	2300	510	2700	510	2900
Two-way	125	220	1600	220	2100	220	2800
	200	520	2650	520	2900	520	3700
	250	720	2800	770	3600	770	4200

Other parameters: $b=2500$ mm, $h=2700$ mm, $f_{cu}=30$ MPa and $\phi=9$ mm

Table 7 Effect of panel height (h) on the pressure and impulse capacity of one- and two-way RC panels

Panel	h (mm)	LD		MD		SD	
		P_0 (kPa)	I_0 (kPa.ms)	P_0 (kPa)	I_0 (kPa.ms)	P_0 (kPa)	I_0 (kPa.ms)
One-way	2700	100	1400	100	1500	100	1700
	3300	50	1350	50	1420	50	1500
	4000	30	1280	30	1380	30	1380
Two-way	2700	220	1600	220	2100	220	2800
	3300	160	1500	160	1800	160	2350
	4000	140	1205	140	1600	140	2200

Other parameters: $b=2500$ mm, $d=125$ mm, $f_{cu}=30$ MPa and $\phi=9$ mm

Table 8 Effect of panel width (b) on the pressure and impulse capacity of one- and two-way RC panels

Panel type	b (mm)	LD		MD		SD	
		P_0 (kPa)	I_0 (kPa.ms)	P_0 (kPa)	I_0 (kPa.ms)	P_0 (kPa)	I_0 (kPa.ms)
One-way	2500	100	1400	100	1500	100	1700
	3400	90	1360	90	1450	90	1510
	4000	85	1300	85	1400	85	1470
Two-way	2500	220	1600	220	2100	220	2800
	3400	170	1400	170	1800	170	2300
	4000	150	1300	150	1600	150	2200

Other parameters: $h=2700$ mm, $d=125$ mm, $f_{cu}=30$ MPa and $\phi=9$ mm

Intensive parametric studies are carried out to investigate the effects of panel RC wall dimensions (height (h), width (b) and depth (d)), concrete strength (f_{cu}) and steel ratio (ρ) on the dynamic response of RC panels as shown in Fig. 8. The numerical results are used to formulate empirical equations that could be easily used to estimate the pressure (P_0) and impulse (I_0) of one- and two-way RC panels have different values of above parameters.

7.1 Dimensions of Panel Wall

The one-and two-way RC panels with wall depths of 125, 200 and 250mm at the same panel width and height of 2500 and 2700mm, respectively, with concrete strength of 30MPa and steel bar diameter of 9mm, were analysed in the present study as shown in Table 6. The outcomes revealed that the resistance capacity of the panel to blast load is significantly improved by increasing its wall depth at the studied damage regions. The maximum increment of the pressure and impulse capacity is observed at a medium damage zone for both types of panels at a depth of 250mm by 410 and 80% in case of a one-way panel, respectively, as well as 250 and 71% in case of two-way panels as compared with a depth of 125 mm. The one-and two-way RC panels with a wall height of 2700, 3300, and 4000mm at

the same panel width and depth of 2500 and 125mm, respectively, with concrete strength of 30MPa and steel bar radius of 9mm, were analysed in the present study as shown in Table 7. In the same context, three wall widths of 2500, 3400 and 4000mm with a wall height of 2700mm were also examined at a similar wall depth, concrete strength and steel ratio shown above to investigate its effects on the panel behaviour as described in Table 8. The results indicated that the resistance capacity of the panel to blast load is reduced by increasing its wall height and width at all the studied damage zones owing to increase the ratio of the panel span to the effective depth and blast load acting on the panel, therefore a significant boost in the deflection was noted. The maximum reduction was observed at the severe damage zone in both types of panel particularly with increased of one-way panel height to 4000mm by 233 and 23% for pressure and impulse, respectively, as compared with height 2700mm.

7.2 Effect of concrete strength (f_{cu})

The strength of concrete utilized in the construction of panel considerably contributed to the shear and ultimate flexural resistance capacity of the panel. Therefore, the one- and two-way RC panels with concrete strength of 25, 30

Table 9 Effect of concrete strength (f_{cu}) on the pressure and impulse of one- and two-way RC panels

Panel type	f_{cu} (MPa)	LD		MD		SD	
		P_0 (kPa)	I_0 (kPa.ms)	P_0 (kPa)	I_0 (kPa.ms)	P_0 (kPa)	I_0 (kPa.ms)
One-way	25	275	1640	275	2300	275	2500
	30	305	2000	305	2500	305	2800
	35	320	2600	320	3000	320	3500
Two-way	25	480	2400	500	2500	500	3500
	30	520	2650	520	2900	520	3700
	35	520	3200	550	3500	550	4000

Other parameters: $b=2500\text{mm}$, $h=2700\text{mm}$, $d=200\text{mm}$ and $\phi=9\text{mm}$

Table 10 Effect of steel reinforcement ratio (ρ) on the pressure and impulse of one- and two-way RC panels

Panel type	ρ	LD		MD		SD	
		P_0 (kPa)	I_0 (kPa.ms)	P_0 (kPa)	I_0 (kPa.ms)	P_0 (kPa)	I_0 (kPa.ms)
One-way	0.0015	90	1300	90	1410	90	1510
	0.0035	100	1400	100	1500	100	1800
	0.0111	110	1650	110	2090	110	2600
Two-way	0.0015	190	1400	200	1800	208	2300
	0.0035	220	1600	220	2100	220	2800
	0.0111	230	1900	230	2500	230	2900

Other parameters: $b=2500\text{mm}$, $h=2700\text{mm}$, $d=125\text{mm}$ and $f_{cu}=30\text{MPa}$

and 35MPa, respectively, were modelled in the current study to evaluate its effects as shown in Table 9. The results demonstrated a notable increase in the panel capacity particularly in term of impulse with maximum increase recorded at a low damage zone of one-way with concrete strength of 35MPa by 59% as compared to a concrete strength of 25MPa. Similar remarks were observed by prior studies (Christian and Chye 2014, Lin *et al.* 2014, Mussa and Mutalib 2018).

7.3 Effect of steel reinforcement ratio (ρ)

Prior studies revealed that the ratio of steel reinforcement has an effective influence on the blast-resistant capacity of the structural member (Lin *et al.* 2014). Hence, different steel ratios of 0.0015, 0.0035 and 0.0111 calculated according to concrete volume in both directions with bars diameter of 6, 9 and 16mm, respectively, were examined to determine its effect on the behaviour of one- and two-way RC panels as given in Table 10. The results indicated that the increase of steel ratio could significantly improve the blast-resistant of the panel especially in term of impulse capacity as noted at severe and medium damage zones of one- and two-way panels with steel ratio of 0.0111 by 72 and 39%, respectively, as compared to the steel ratio of 0.0015.

8. Formulation of P-I diagrams equations

Empirical formulae are derived to predict the P-I diagrams of one- and two-way RC panels with different panel dimensions, concrete strength and steel reinforcement

ratio at different damage levels by using the least-squares fitting method. The value of constant (A) was found to be 0.25 to achieve an accurate prediction for the P-I diagrams of one- and two-way RC panel as described below. A similar approach was adopted by prior study (Shope 2007).

8.1 One-way panel

The value of constant (β) was considerably varied according to parametric studies results and mainly depended on the pressure and impulse asymptotes as follows:

$$\beta = 1.37 + 7.4 \times 10^{-4} P_0 + \frac{2.87 \times 10^3}{I_0} - \frac{4.45 \times 10^6}{I_0^2} + \frac{2.49 \times 10^9}{I_0^3} \quad (5)$$

$$\beta \geq 2 \text{ for the one-way panel.}$$

Based on numerical results and least-squares fitting, the pressure (P_0) and impulse (I_0) at different damage levels are calculated as follows:

$$P_0(LD) = 4.5f_{cu} + 3.06d - 0.00264b - 0.0415h + 890.06\rho - 309.193 \quad (6)$$

$$I_0(LD) = 96f_{cu} + 8.54d - 0.0529b - 0.0552h + 7716.8\rho - 2365.31 \quad (7)$$

$$P_0(MD) = 4.5f_{cu} + 3.06d - 0.00264b - 0.0415h + 890.06\rho - 309.193 \quad (8)$$

Table 11 Comparison between the results of numerical and proposed equations to calculate the pressure and impulse of one-way RC panel (P1)

Panel	Results	LD		MD		SD	
		P_0 (kPa)	I_0 (kPa.ms)	P_0 (kPa)	I_0 (kPa.ms)	P_0 (kPa)	I_0 (kPa.ms)
P1	Numerical	100	1400	100	1500	100	1700
	Proposed Formula	93	1328	93	1380	93	1777
	$Error = \left \frac{Proposed - Numerical}{Numerical} \right \times 100$	7	5	7	8	7	5
Other parameters: $b=2500\text{mm}$, $h=2700\text{mm}$, $d=125\text{mm}$, $f_{cu}=30\text{MPa}$, $\phi=9\text{mm}$							

Table 12 Comparison between the results of numerical and proposed equations to calculate the pressure and impulse of two-way RC panel (P3)

Panel	Results	LD		MD		SD	
		P_0 (kPa)	I_0 (kPa.ms)	P_0 (kPa)	I_0 (kPa.ms)	P_0 (kPa)	I_0 (kPa.ms)
P3	Numerical	220	1600	220	2100	220	2800
	Proposed Formula	204	1536	204	1905	207	2624
	$Error = \left \frac{Proposed - Numerical}{Numerical} \right \times 100$	7	4	7	9	6	6
Other parameters: $b=2500\text{mm}$, $h=2700\text{mm}$, $d=125\text{mm}$, $f_{cu}=30\text{MPa}$, $\phi=9\text{mm}$							

$$I_0(MD) = 70f_{cu} + 12.859d - 0.065b - 0.067h + 16395.28\rho - 2041.896 \quad (9)$$

$$P_0(LD) = 4.0f_{cu} + 4.058d - 0.0477b - 0.04903h + 715.048\rho - 173.997 \quad (13)$$

$$P_0(SD) = 4.5f_{cu} + 3.049d - 0.0032b - 0.042h + 605.32\rho - 303.086 \quad (10)$$

$$I_0(LD) = 80f_{cu} + 13.059d - 0.236b - 0.222h + 9028.10\rho - 1339.340 \quad (14)$$

$$I_0(SD) = 100f_{cu} + 14.187d - 0.174b - 0.188h + 25631.67\rho - 2142.363 \quad (11)$$

$$P_0(MD) = 5.0f_{cu} + 4.319d - 0.04781b - 0.04912h + 672.996\rho - 235.585 \quad (15)$$

where P_0 in kPa, I_0 in kPa.ms, f_{cu} in MPa, and h , b and d in mm. The accuracy of the proposed formula was validated with the numerical results of RC panel (P1) as shown in Table 11 and Fig. 9. The results proved the high accuracy of the proposed formulae to predict the P-I curves of one-way RC panel at different damage levels within maximum absolute error in pressure and impulse by 7 and 8%, respectively, as compared with the numerical approach. It should be noted that the equivalent steel area (A_{se}) defined in Equation 2 has to be used when calculating the respective reinforcement ratio.

8.2 Two-way panel

Similarly, the (β) value for the two-way panel is derived as:

$$\beta = 2.24 - 38P_0 - \frac{4.84 \times 10^2}{I_0} + \frac{1.42 \times 10^6}{I_0^2} - \frac{1.03 \times 10^9}{I_0^3} \quad (12)$$

$$\beta \geq 2$$

The empirical formulae for the P_0 and I_0 at different damage levels are given below, in which I_0 in kPa.ms and P_0 in kPa and h , b and d in mm:

$$I_0(MD) = 100f_{cu} + 13.095d - 0.297b - 0.251h + 15099.892\rho - 1364.789 \quad (16)$$

$$P_0(SD) = 5.0f_{cu} + 4.296d - 0.04954b - 0.05067h + 582.33\rho - 221.37 \quad (17)$$

$$I_0(SD) = 50f_{cu} + 13.535d - 0.39574b - 0.32525h + 8674.34\rho - 1269.21 \quad (18)$$

Table 12 and Fig. 10 proved the capability of the proposed empirical formula to predict the P-I diagrams of two-way RC panel (P3) within maximum absolute error in pressure and impulse by 7 and 9%, respectively. Accordingly, the proposed equations will significantly help the designers in prediction the damage level of RC panels within a high accuracy to provide an appropriate protection for these structures under blast loads.

6. Conclusion

A numerical model is developed to predict the dynamic response and damage of RC panels under blast loading. The

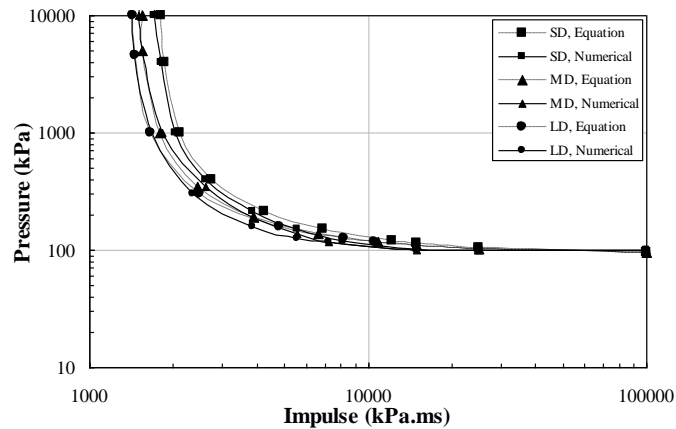


Fig. 9 Comparison of P-I curves determined by numerical and proposed formulae for one-way RC panel (P1)

Other parameters: $b=2500\text{mm}$, $h=2700\text{mm}$, $d=125\text{mm}$, $f_{cu}=30\text{MPa}$, $\phi=9\text{mm}$

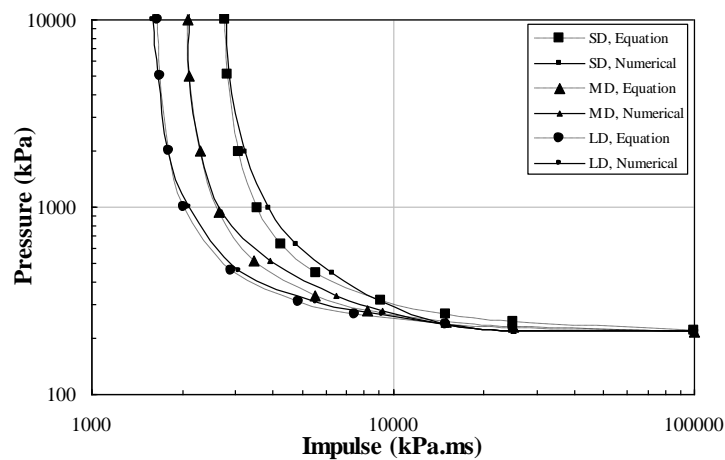


Fig. 10 Comparison of P-I curves determined by numerical and proposed formulae for two-way RC panel (P3)

Other parameters: $b=2500\text{mm}$, $h=2700\text{mm}$, $d=125\text{mm}$, $f_{cu}=30\text{MPa}$, $\phi=9\text{mm}$

accuracy of this model is verified with previous experimental test and revealed a good consistency in terms of displacement and failure at most the investigated locations with an absolute average error of 4%. The mechanism analysis of failure indicated that the one- and two-way RC panel might be failed within four modes. The shear failure was dominant at the impulsive region in both panel cases within a blast pressure of 15000kpa and an impulse range of 2000 to 2400kpa.ms. The flexural damage of panel is started to appear via decrease of blast pressure and increase its impulse, where a combination of shear and flexural failure was observed at a pressure of 5000kpa and an impulse range of 2100 to 3000kpa.ms. The flexural deflection is totally governed by the dynamic region at the blast pressure of 1000kpa and an impulse range of 2500 to 4500kpa.ms. An obvious transverse shear failure at the support was observed at the quasi-static region when the pressure is further decreased to a range of 125 to 230kpa and the blast impulse is increased to 15000kpa.ms. The empirical study proved that the hyperbolic equation is the most appropriate to predict the P-I curves of one- and two way RC panels within identical damage levels as stated by

UFC-3-340-02 (2008). The parametric studies results proved that the dimensions of the panel RC wall, concrete strength, and steel reinforcement ratio could considerably affect the blast resistance capacity of the panel. Therefore, empirical formulae were proposed in terms of the above parameters to predict the P-I curve of the one- and two-way panels within a high accuracy as compared with numerical results. The proposed equations will provide the designers with significant information about panel safety under different blast loads.

Acknowledgements

The authors would like to thank the Research University Grant (GUP-2018-029) and Fundamental Research Grant Scheme (FRGS/1/2015/TK01/UKM/02/4) for their financial support in order to accomplish the current research.

References

Alamatian, J. (2013), "New implicit higher order time integration for dynamic analysis", *Struct. Eng. Mech.*, **48**(5), 711-736.

- <https://doi.org/10.12989/sem.2013.48.5.711>.
- Abbood, I. S., Mahmood, M., Hanoon, A. N., Jaafar, M. S. and Mussa, M. H. (2018), "Seismic response analysis of linked twin tall buildings with structural coupling", *IJCIET*, **9**(11), 208-219.
- Abedini, M., Mutalib, A. A., Raman, S. N., Akhlaghi, E., Mussa, M. H. and Ansari, M. (2017), "Numerical investigation on the non-linear response of reinforced concrete (RC) columns subjected to extreme dynamic loads", *J. Asian Sci. Res.*, **7**(4), 86. <https://doi.org/10.18488/journal.2.2017.74.86.98>.
- Aghdamy, S., Wu, C. and Griffith, M. (2013), "Simulation of retrofitted unreinforced concrete masonry unit walls under blast loading", *Int. J. Prot. Struct.*, **4**(1), 21-44. <https://doi.org/10.1260%2F2041-4196.4.1.21>.
- CEB-FIP, M. (1993), Design of Concrete Structures, British Standard Institution; London, United Kingdom.
- Christian, A. and Chye, G.O. (2014), "Performance of fiber reinforced high-strength concrete with steel sandwich composite system as blast mitigation panel", *Procedia Eng.*, **95**, 150-157. <https://doi.org/10.1016/j.proeng.2014.12.174>.
- Gebbekken, N. and Ruppert, M. (1999), "On the safety and reliability of high dynamic hydrocode simulations", *Int. J. Numer. Meth. Eng.*, **46**(6), 839-851. [https://doi.org/10.1002/\(SICI\)1097-0207\(19991030\)46:6%3C839::AID-NME728%3E3.0.CO;2-R](https://doi.org/10.1002/(SICI)1097-0207(19991030)46:6%3C839::AID-NME728%3E3.0.CO;2-R).
- Ha, J. H., Yi, N. H., Choi, J. K. and Kim, J. (2011), "Experimental study on hybrid CFRP-PU strengthening effect on RC panels under blast loading", *Compos. Struct.*, **93**(8), 2070-2082. <https://doi.org/10.1016/j.compstruct.2011.02.014>.
- Hou, X., Cao, S., Rong, Q. and Zheng, W. (2018), "A PI diagram approach for predicting failure modes of RPC one-way slabs subjected to blast loading", *Int. J. Impact Eng.*, **120**, 171-184. <https://doi.org/10.1016/j.ijimpeng.2018.06.006>.
- Krajcinovic, D. (1972), "Clamped circular rigid-plastic plates subjected to central blast loading", *Comput. Struct.*, **2**(4), 487-496. [https://doi.org/10.1016/0045-7949\(72\)90003-X](https://doi.org/10.1016/0045-7949(72)90003-X).
- Krauthammer, T., Astarlioglu, S., Blasko, J., Soh, T. and Ng, P. (2008), "Pressure-impulse diagrams for the behavior assessment of structural components", *Int. J. Impact Eng.*, **35**(8), 771-783. <https://doi.org/10.1016/j.ijimpeng.2007.12.004>.
- Lee, H.K. and Kim, S.E. (2016), "Comparative assessment of impact resistance of SC and RC panels using finite element analysis", *Prog. Nuclear Energy*, **90**, 105-121. <https://doi.org/10.1016/j.pnucene.2016.03.002>.
- Lin, X., Zhang, Y. and Hazell, P.J. (2014), "Modelling the response of reinforced concrete panels under blast loading", *Mater. Des.*, **56**, 620-628. <https://doi.org/10.1016/j.matdes.2013.11.069>.
- Lin, X. and Zhang, Y. (2016), "Nonlinear finite element analysis of FRP-strengthened reinforced concrete panels under blast loads", *Int. J. Comput. Methods*, **13**(04), 1641002. <https://doi.org/10.1142/S0219876216410024>.
- LSTC, L.D. (2012), Keyword Users Manual: Volume I, V971 R6.0, Livermore, CA: Livermore Technology Software Corporation; USA.
- Malvar, L.J., Crawford, J.E., Wesevich, J.W. and Simons, D. (1997), "A plasticity concrete material model for DYNA3D", *Int. J. Impact Eng.*, **19**(9-10), 847-873. [https://doi.org/10.1016/S0734-743X\(97\)00023-7](https://doi.org/10.1016/S0734-743X(97)00023-7).
- Malvar, L.J. (1998), "Review of static and dynamic properties of steel reinforcing bars", *Mater. J.*, **95**(5), 609-616.
- Malvar, L.J. and Ross, C. A. (1998), "Review of strain rate effects for concrete in tension", *ACI Mater. J.*, **95**, 735-739.
- Mendes, S. and Opat, H. (1973), "Tearing and shear failures in explosively loaded clamped beams", *Exp. Mech.*, **13**, 480-486.
- Mussa, M.H., Mutalib, A.A., Hamid, R., Naidu, S.R., Radzi, N.A. M. and Abedini, M. (2017), "Assessment of damage to an underground box tunnel by a surface explosion", *Tunn. Undergr. Space Technol.*, **66**, 64-76. <https://doi.org/10.1016/j.tust.2017.04.001>.
- Mussa, M. H., Mutalib, A. A., Hamid, R. and Raman, S. N. (2018), "Dynamic properties of high volume fly ash nanosilica (HV-FANS) concrete subjected to combined effect of high strain rate and temperature", *Lat. Am. J. Solids Struct.*, **15**(1). <https://doi.org/10.1590/1679-78254900>.
- Mussa, M. H. and Mutalib, A. A. (2018), "Effect of geometric parameters (β and τ) on behaviour of cold formed stainless steel tubular X-joints", *Int. J. Steel Struct.*, **18**(3), 821-830. <https://doi.org/10.1007/s13296-018-0031-0>.
- Mussa, M. H., Mutalib, A. A., Hamid, R. and Raman, S. N. (2018), "Blast damage assessment of symmetrical box-shaped underground tunnel according to peak particle velocity (PPV) and single degree of freedom (SDOF) criteria", *Symmetry*, **10**(5), 158. <https://doi.org/10.3390/sym10050158>.
- Mussa, M. H., Abdulhadi, A. M., Abbood, I. S., Mutalib, A. A. and Yaseen, Z. M. (2020), "Late age dynamic strength of high-volume fly ash concrete with nano-silica and polypropylene fibres", *Crystals*, **10**(4), 243. <https://doi.org/10.3390/cryst10040243>.
- Muszynski, L. C. and Purcell, M. R. (2003), "Composite reinforcement to strengthen existing concrete structures against air blast", *J. Composite Constr.*, **7**(2), 93-97. [https://doi.org/10.1061/\(ASCE\)1090-0268\(2003\)7:2\(93\)](https://doi.org/10.1061/(ASCE)1090-0268(2003)7:2(93)).
- Mutalib, A. A. and Hao, H. (2011), "Development of PI diagrams for FRP strengthened RC columns", *Int. J. Impact Eng.*, **38**(5), 290-304. <https://doi.org/10.1016/j.ijimpeng.2010.10.029>.
- Mutalib, A. A., Mussa, M. H. and Abdulghafoor, A. M. (2018), "Finite element analysis of composite plate girders with a corrugated web", *J. Eng. Sci. Technol.*, **13**(9), 2978-2994.
- Mutalib, A. A., Mussa, M. H. and Abusal, K. M. (2018), "Numerical evaluation of concrete filled stainless steel tube for short columns subjected to axial compression load", *J. Teknol.*, **80**(2).
- Mutalib, A. A., Mussa, M. H. and Hao, H. (2019), "Effect of CFRP strengthening properties with anchoring systems on PI diagrams of RC panels under blast loads", *Constr. Build. Mater.*, **200**, 648-663. <https://doi.org/10.1016/j.conbuildmat.2018.12.169>.
- Mutalib, A. A., Mussa, M. H. and Taib, M. A. (2020), "Behaviour of prestressed box beam strengthened with CFRP under effect of strand snapping", *GRADEVINAR*, **72**(2), 103-113. <https://doi.org/10.14256/JCE.2368.2018>.
- Ngo, T. D. (2005), "Behaviour of high strength concrete subject to impulsive loading", Ph.D. Dissertation, The University of Melbourne, Melbourne, Australia.
- Ngo, T., Mendis, P., Gupta, A. and Ramsay, J. (2007), "Blast loading and blast effects on structures-an overview", *Electron. J. Struct. Eng.*, **7**(S1), 76-91.
- Nurick, G. and Shave, G. (1996), "The deformation and rupture of blast loaded square plates", *Int. J. Impact Eng.*, **18**, 99-116.
- Olson, M., Nurick, G. and Fagnan, J. (1993), "Deformation and rupture of blast loaded square plates-predictions and experiments", *Int. J. Impact Eng.*, **13**(2), 279-291. [https://doi.org/10.1016/0734-743X\(93\)90097-Q](https://doi.org/10.1016/0734-743X(93)90097-Q).
- Oswald, C. and Marchand, K. (1994), Facility and Component Explosive Damage Assessment Program (FACEDAP): Theory manual, Southwest Research Institute for the Department of the Army; Omaha, USA.
- Parlin, N. J., Davids, W. G., Nagy, E. and Cummins, T. (2014), "Dynamic response of lightweight wood-based flexible wall panels to blast and impulse loading", *Constr. Build. Mater.*, **50**, 237-245. <https://doi.org/10.1016/j.conbuildmat.2013.09.046>.
- Riedel, W., Mayrhofer, C., Thoma, K. and Stolz, A. (2010), "Engineering and numerical tools for explosion protection of reinforced concrete", *Int. J. Prot. Struct.*, **1**(1), 85-101. <https://doi.org/10.1260%2F2041-4196.1.1.85>.
- Saadun, A., Mutalib, A. A., Hamid, R. and Mussa, M. H. (2016),

- “Behaviour of polypropylene fiber reinforced concrete under dynamic impact load”, *J. Eng. Sci. Technol.*, **11**(5), 684-693.
- Scherbatiuk, K., Rattanawangcharoen, N., Pope, D. and Fowler, J. (2008), “Generation of a pressure-impulse diagram for a temporary soil wall using an analytical rigid-body rotation model”, *Int. J. Impact Eng.*, **35**(6), 530-539. <https://doi.org/10.1016/j.ijimpeng.2007.04.006>.
- Shen, J., Lu, G., Wang, Z. and Zhao, L. (2010), “Experiments on curved sandwich panels under blast loading”, *Int. J. Impact Eng.*, **37**(9), 960-970. <https://doi.org/10.1016/j.ijimpeng.2010.03.002>.
- Shi, Y., Hao, H. and Li, Z.-X. (2008), “Numerical derivation of pressure-impulse diagrams for prediction of RC column damage to blast loads”, *Int. J. Impact Eng.*, **35**(11), 1213-1227. <https://doi.org/10.1016/j.ijimpeng.2007.09.001>.
- Shi, Y., Li, Z.-X. and Hao, H. (2009), “Bond slip modelling and its effect on numerical analysis of blast-induced responses of RC columns”, *Struct. Eng. Mech.*, **32**(2), 251-267. <http://dx.doi.org/10.12989/sem.2009.32.2.251>.
- Shi, Y. and Stewart, M. G. (2015), “Spatial reliability analysis of explosive blast load damage to reinforced concrete columns”, *Struct. Saf.*, **53**, 13-25. <https://doi.org/10.1016/j.strusafe.2014.07.003>.
- Shope, R. (2007), “Comparisons of an alternative pressure-impulse (P-I) formulation with experimental and finite element results”, *The International Symposium on the Effects of Munitions with Structures (ISIEMS)*, Orlando, USA, November.
- Sohn, J. M., Kim, S. J., Seong, D. J., Kim, B. J., Ha, Y. C., Seo, J. K. and Paik, J. K. (2014), “Structural impact response characteristics of an explosion-resistant profiled blast walls in arctic conditions”, *Struct. Eng. Mech.*, **51**(5), 755-771. <https://doi.org/10.12989/sem.2014.51.5.755>.
- Syed, Z. I., Mendis, P., Lam, N. and Ngo, T. (2006), “Concrete damage assessment for blast load using pressure-impulse diagrams”, *Proceedings of Annual Technical Conference of the Australian Earthquake Engineering Society*, Canberra, Australia, November.
- Teeling-Smith, R. and Nurick, G. (1991), “The deformation and tearing of thin circular plates subjected to impulsive loads”, *Int. J. Impact Eng.*, **11**(1), 77-91. [https://doi.org/10.1016/0734-743X\(91\)90032-B](https://doi.org/10.1016/0734-743X(91)90032-B).
- UFC-3-340-02 (2008), Structures to resist the effects of accidental explosions, US Army Corps of Engineers, Naval Facilities Engineering Command; Washington DC, USA.
- Wu, C. and Hao, H. (2005), “Modeling of simultaneous ground shock and airblast pressure on nearby structures from surface explosions”, *Int. J. Impact Eng.*, **31**(6), 699-717. <https://doi.org/10.1016/j.ijimpeng.2004.03.002>.
- Xia, Y., Wu, C., Zhang, F., Li, Z.-X. and Bennett, T. (2014), “Numerical analysis of foam-protected RC members under blast loads”, *Int. J. Prot. Struct.*, **5**(4), 367-390. <https://doi.org/10.1260/2F2041-4196.5.4.367>.
- Yonten, K., Manzari, M. T., Eskandarian, A. and Marzougui, D. (2002), “An evaluation of constitutive models of concrete in LS-Dyna finite element code”, *15th ASCE Engineering Mechanics Conference*, New York, USA, June.
- Yu, R., Chen, L., Fang, Q., Yan, H. and Chen, G. (2019), “Generation of pressure-impulse diagrams for failure modes of RC columns subjected to blast loads”, *Eng. Failure Anal.*, **100**, 520-535. <https://doi.org/10.1016/j.engfailanal.2019.02.001>.